ОБЪЕДИНЕННЫЙ
ИНСТИТУТ
ЯДЕРНЫХ
ИССЛЕДОВАНИЙ

Дубна

E3-99-146

E.P.Grigoriev*, V.A.Khitrov, A.M.Sukhovoj,
E.V.Vasilieva

A SEARCH FOR THE γ-DECAY OF THE ^{168}Er COMPOUND NUCLEUS IN THE $(n, 2\gamma)$ REACTION

Submitted to «Fizika B»

*Research Institute of Physics, St.-Petersburg State University, Russia

1999

1 Introduction

The structure of the ^{168}Er even-even deformed nucleus has been well studied in complex experiments [1,2] and analysed from the model point of view [3]. The excitation of the states of this nucleus was studied in different nuclear processes, first of all — in the (n,γ) reaction using the best apparatus of 1980-1990s: magnetic β-spectrometers, and semiconductor and crystal-diffraction γ-spectrometers. In this reaction, the spectrum of γ-transitions was measured for the intervals $E_\gamma < 2.52$ keV and $4.62 < E_\gamma < 7.7$ MeV (B_n=7.771 MeV). These experimental data allowed the authors of [1,2] to conclude that the levels of this nucleus were established (probably, partially) up to the excitation energy of 3.14 MeV and the complete decay scheme up to $E_{ex} < 2.6$ MeV. The parameters of more than 30 rotational bands were determined, as well.

Further experiments, however, have shown that real situation in ^{168}Er differs from the model notions. Recent measurements of the $\gamma\gamma$-coincidences in the (n,γ) reaction [4,5] stipulated the necessity of introducting a number of new excited levels of ^{168}Er in the diapason from 2.19 to 2.97 MeV. It was shown that some number of γ-transitions cannot depopulate the levels to which they were assigned in accordance with the combinatorial rule. As follows from the data on the $(n,n'\gamma)$ reaction [6], the three levels: 2133 keV ($J^\pi = 1^+$), 2177 keV (2^+), and 2365 keV (1), were introduced by mistake. Authors of [6] made the depopulation of some other states more precise and showed that the mechanism of the $(n,n'\gamma)$ reaction corresponds to the predictions of the statistical model.

Experimental study of the two-step γ-cascades and analysis of spectroscopic information performed by us allowes one to verify the known decay scheme of ^{168}Er and extend it above the excitation energy of 2.5 MeV. The use of the method [7] of joint analysis of the spectroscopic data on the (n,γ) and $(n,2\gamma)$ reactions (i.e., of the data obtained in single-detector measurements and in two-detector sum-coincidence measurements) allowed some grounded conclusions to be made about:

(a) the presence of unresolved doublets of levels and transitions;

(b) the degree of completeness of a set of transitions depopulating a given level.

2 Experiment and data analysis

The method of the experiment and data analysis (called below the "$(n,2\gamma)$ reaction") used by us is described in detail in [8,9]. Its distinctions from the traditional analysis of the $\gamma\gamma$-coincidences are the following:

(a) from the mass of coinciding pairs of γ-transitions, only those whose sum energies exceed a sufficiently high value are selected and accumulated for the further analysis. In the present experiment, this threshold was set at 5 MeV and, to reject annihilation quanta, the detection threshold for each transition was set at 520 keV;

(b) the spectra are built from events satisfying the condition $B_n - E_f - \delta < E_1 + E_2 < B_n - E_f + \delta$. The width and position of the corresponding interval 2δ are unambiguously determined from the sum coincidence spectrum. In the other words, one selects from the three-dimensional space "number of events - E_1 - E_2", if using traditional analysis, the coincidences within the "corridor" that is parallel to one of the energies, then the method used by us uses the same, but along the diagonal $E_1 = (B_n - E_f) - E_2$. This allows us:

(1) to select events from that region of the three-dimensional space which is characterized by the minimum possible background;

(2) to use numerical method [10] for improving the energy resolution without decreasing the efficiency of registration;

(3) to subtract the background from the spectra in an effective and reliable way, built in an "off-line" regime;

(4) to concentrate a maximum number of peaks of cascade transitions into a minimum number of spectra at a fixation of both initial and final cascade levels, and to distinguish the continuous components of spectra, which are related to a great number of low-intensity cascades;

(5) by means of the maximum likelihood method, to determine unambiguously and independently the quanta ordering in the majority of the observed cascades of dipole transitions with the sum energy of several MeV. Modern experimental technique allows one to do this for a very limited set of cases.

The experiment was performed at the IBR-30 pulsed reactor in Dubna. The $\gamma\gamma$-coincidences were registered by a system of two 7-10% efficiency Ge(Li) detectors for about 400 hours. The advantages of our method mentioned above permitted us to obtain information which is not less than that accumulated by authors of [5] by means of a TESSA array using 16 Compton-supressed Ge detectors over a 4-day period at the neutron beam of the BNL reactor.

3 Experimental results

3.1 Decay scheme

The bulk of the information on cascade γ-transitions obtained within the sum coincidence technique is limited, first, by background conditions which are related to the registration of events by Ge detectors in a continuous distribution but not in full energy peaks. For this reason, it was possible to obtain only the spectra of two-step cascades proceeding between the compound state and the following low-lying levels of ^{168}Er: 79.80 keV (2^+), 264.09 keV (4^+), 548.75 keV (6^+), 821.17 keV (2^+_γ), 895.80 keV (3^+_γ), 994.75 keV (4^+_γ), and 1094.04 keV (4^-), i.e., the spectra of cascades terminating at the three levels of the rotational band of the ground state, three levels of the γ-band, and the head level of the band $K^\pi = 4^-$.

The energies of these levels and the value $B_n = 7771.15$ keV were used for calibrating the energy scale. The absolute intensities (in % per decay) of all cascades were determined with the help of a normalization of the relative intensities of the strongest cascades to their absolute values $i_{\gamma\gamma}$, which were calculated by equation

$$i_{\gamma\gamma} = i_1 \times BR. \qquad (1)$$

Here, the absolute intensities i_1 of the corresponding primary transitions were obtained using their relative values from [1,2] and the normalizing multiplier 0.02 from [4]; the branching ratios $BR = i_2 / \sum i_2$ were determined in a standard way from the spectra of secondary transitions coinciding with the same set of primary transitions. To obtain the BR values, we used all the mass of coincidences registered in present experiment.

The total intensity of all two-step cascades observed in the experiment (including those unresolved experimentally) is equal to 37(4)%.

The mean error in the determination of the energies of the cascade transitions was about 1.55 keV. For this reason, in Tables 1 and 2, which summarize the information on the decay scheme of ^{168}Er accumulated by us, the energies of the secondary transitions determined in present experiment are replaced by more precise data [1]. According to [7], this was performed by accounting for not only the differences between the transition energies obtained by us and authors of [1], but also the relations between the intensities of cascades and their low-energy secondary transitions. The necessity of testing these relations is due to two reasons. First, this permits one to control the correctness of the assignment of the energy values. Second, this provides an opportunity to verify the data [1] in order to reveal the doublets of unresolved transitions. If the ratios $r = i_{\gamma\gamma}/i_2$ for the cascades proceeding via the same intermediate level are in agreement within the experimental errors, then one can conclude that transition chosen from data [1] is the one that depopulates a given level and that it is not a doublet. It is obvious that the cascade intensity must not exceed the intensities of the corresponding primary and secondary transitions from [1] which are compared to those obtained by us.

If this is not so, then (for the primary transitions) either the intensity of the high-energy transition from [1] was determined with an error or, for some reason, the data on energies and intensities of cascades obtained by us contain an error. Potential errors in our data, however, can be due to only possibility: the energy of the secondary quantum in the cascade of 3 and more γ-transitions coincides with the difference of the energies of a pair of lower-lying levels to a precision of 3-4 keV, and this (i.e., third) transition must be dominant in the γ-decay of the intermediate level excited by the preceding transition. Just such a situation, most probably, is observed for the cascades with the 1633 and 1905 keV intermediate levels. However, we cannot explain, in the same way, the surplus in the intensities of the cascades proceeding through the 895, 1995, and 3011 keV intermediate levels. This discrepancy requires another explanation. One cannot exclude, for example, the possible influence of interference effects on the intensity of primary transitions — the effective energy of captured neutrons in different experiments can be different. The most probable explanation, however, is that due to poor statistics, we observed a random divergence in our experiment which is several times larger than the estimation of the statistical error.

A distribution of the ratios of the sum cascade intensities to the intensity of their common primary transition $r = \sum i_{\gamma\gamma}/i_1$ is shown in Fig. 1. The mean with respect to 91 intermediate cascade levels is $< r >= 0.83$. This means that the sum intensity of the secondary transitions listed in Table 1 amounts to 83% of their total value. The remaining 17% are related to the cascades with $i_{\gamma\gamma} \leq 10^{-4}$ terminating at the 7 levels mentioned in the beginning of this paragraph or to cascades to the ground state or to levels at $E_f > 1.1$ MeV. Figure 1 and Table 1 determine quite unambiguously those states of ^{168}Er whose decay modes were established incompletely. Certainly, the r value is affected by the uncertainty in determination of a given above coefficient of transition from the relative [4] to absolute intensities. Corresponding error can be estimated at the level of $\sim 10\%$. The r values found for each levels listed in Table 1 allows considerable reduction of false placing of γ-transitions with close energies into the decay scheme.

Essential information about the mechanism of reaction of the slow neutron radiative

capture can be derived from the comparison of the experimental and model calculated ratios $i_{\gamma\gamma}/i_2$ (10th column in Table 1). In turn, this value determines the ratio between the intensities of the direct primary transition and a number of cascades with several transitions, which populate the same state E_i. The necessity of such analysis follows from the data shown in Figs. 4 and 5 which demonstrate considerable discrepancy between the model notions of a nucleus and experimental situation.

3.2 Verification of the existing decay scheme and new modes of decay

Comparing our data on the decay scheme of ^{168}Er with those from [1,2], one can conclude that the information on both the decay modes on the whole and the sufficiently precise established decay ways of levels above the excitation energy of about 2.5 MeV is first obtained by us. Our data on the decay scheme of ^{168}Er are listed in Tables 1 and 2. But a matter of larger interest are the cases when, on the grounds of the data on two-step cascades, one can determine the incorrect placement of transitions in the known decay scheme.

Such cases were not found below the excitation energy of 2 MeV although we did not observe several cascades whose probable secondary transitions were placed in the decay scheme [1,2]. So, we did not observe the three strongest cascades whose 915, 1413, and 1076 keV secondary transitions depopulate, according to [1,2], intermediate levels at 994, 1493, and 1972 keV, respectively. These cascades must have intensity about 10^{-4} per decay. However, this value is close to the registration threshold L_c in our experiment or even less than it.

In the excitation energy interval 2.0 to 2.4 MeV, we did not observe cascade with a 1407 keV secondary transition ($E_i = 2302.68$ keV) and $i_{\gamma\gamma} = (1-2) \times 10^{-4}$. At the same time, the data on cascades permitted us to introduce 8 more levels into the decay scheme for this energy interval. This allows the following conclusion: the existing [2] decay scheme of ^{168}Er below $E_i \simeq 2.4$ MeV has been established with maximum high reliability, at least for the most intense transitions observed in the (n,γ) reaction.

3.3 Estimation of completeness of the system of established levels

The presence of the registration threshold for individual transitions or cascades, together with the problems concerning the reconstruction of a decay scheme on the basis of experimental spectra motivate the necessity of finding a method of estimating the number of missing levels. Some conclusions about this problem can be made in the following way — all two-step cascade spectra consist of:

(a) a number of well-resolved discrete peaks corresponding to cascades with $i_{\gamma\gamma} > L_c$ (background peaks appear in these spectra in very small quantity, in very specific cases, and they can be easily identified);

(b) a continuous, low amplitude distribution related to the large number of low-intensity ($i_{\gamma\gamma} < L_c$) cascades;

(c) a "noise" line with zero mean value (result of subtracting the background).

As a result of (a), the existing set of cascades (Table 1 and, probaly, Table 2) practically does not contain false data and can be considered as a "complete" statistical ensemble of random values which have some distribution for intensities $i_{\gamma\gamma} > L_c$. The L_c value for cascades is determined only by the experimental conditions (i.e., by condition (c)). For the data listed in Tables 1 and 2, $L_c \simeq (1-2) \times 10^{-4}$ per decay of the compound state.

There is no reliable information on the shape of the intensity distribution of primary transitions and, all the more so, of those cascades which excite intermediate levels of even-even deformed nuclei in the interval, for example, $2.0 < E_i < 3.5$ MeV. The matrix element of primary transitions at the γ-decay of neutron resonance is the sum of a large number of random items (in the frame of the existing theoretical notions of the structure of nuclear levels and the probabilities of transitions between them). Accounting for this, one can expect that, in the first approach, the divergences of cascade primary transitions with respect to the mean value are described by the Porter-Thomas distribution [12]. As mentioned above, the sum $\sum i_{\gamma\gamma}$ of the cascade intensities measured in the experiment is rather close to that of their primary transitions, i.e., the distribution of this sum is like the random distribution of i_1.

On this basis, we compared the Porter-Thomas distributions (with the parameters providing the best agreement with the experiment) and the sum intensities of cascades (which excite the same intermediate level) in order to estimate a number of missing levels in ^{168}Er. Cumulative sums of the experimental (histograms) and simulated within the Porter-Thomas distribution (curves) cascade intensities for the 0.5 MeV intervals in the excitation energy diapason 1.5 to 4 MeV are shown in Fig. 2.

The results of this comparison are given in Table 3, as well as the results of an analogous analysis performed for primary transitions from [2]. When considering these results, one should take into account that the process under study is affected by the structure of the matrix element of the primary transition — the presence of one or more items which considerably exceed other components must decrease (in comparison with predictions of [12]) the number of low-intensity cascades (transitions) and increase the number of intense cascades.

Therefore, the obtained δI and δN values should be considered only as upper estimates. Nevertheless, one should expect the presence, as a minimum, of 10 to 15 unknown levels in the 1.5 to 2.5 MeV excitation interval of ^{168}Er.

At higher excitation energies, the situation is radically different. On the one hand, a rather good description of cumulative sums of the experimental cascade intensities for $i_{\gamma\gamma} > L_c$ by the Porter-Thomas distribution (corresponding numbers of degrees of freedom N_i^{mod} are listed in Table 3) allows us to hope for correct extrapolation to the $i_{\gamma\gamma} < L_c$ region. On the other hand, the data of Table 3 unambiguously require one to refuse the conventional notion of an exponential increase in the level density when the excitation energy increases (the exponential law is the basic idea for level density models like such as the back-shifted Fermi-gas model with parameters from [14]).

There are apparently only two solutions of this problem. The first: we have no grounds to exclude the potential possibility of the coexistence of two or more systems of nuclear levels (with $J = 2-5$ in the case of the nucleus under study) above a nuclear excitation energy of 2.0-2.5 MeV. These systems can include different numbers of states and their excitation probabilities can differ, at least, by a factor of 100 or more. (When modelling the distributions shown in Fig. 2, we accounted for the fact that cascades with $E1$ and $M1$

primary transitions have different but comparable (the Δ value in Table 3) intensities). A potential discrepancy in excitation probabilities can appear only for the cascades with $i_{\gamma\gamma} < L_c$. This statement is motivated by analysis of the data listed in Table 3 and plotted in Fig. 4. The joint interpretation of these data is possible only in the framework of the assumption that the number of the cascade intermediate levels appearing in the energy interval from 2 to 4 MeV of ^{168}Er is almost constant and the discrepancy between the experiment and exponential extrapolation of the level density cannot be explained by the traditional "omission" of weakly excited states.

The alternative to this conventional notion is a different type of the dependence on energy for the density of states excited after thermal neutron capture in the ^{167}Er target-nucleus. The method providing realistic estimation of level density from the measurements of the $(n, 2\gamma)$ reaction was first described in [15]. Further development of this method allows us to estimate both the level density and sums of the strength functions

$$f = < \Gamma_{\lambda i} > /(E_\gamma^3 \times A^{2/3} \times D_\lambda) \qquad (2)$$

(partial widths) of dipole $E1$ and $M1$ transitions by means of modelling complete sets of their most probable values in the framework of numerical solution of equations which determine:

(a) experimental value of the total radiative width of the ^{168}Er compound state: $\Gamma_\lambda = \sum_i \Gamma_{\lambda i} \times (\rho \Delta E) = 88(2)$ meV [16];

(b) dependence of the cascade intensity on the excitation energy of their intermediate levels (Fig. 3).

As can be seen from Fig. 4, exponential extrapolation [14] does not allow one to calculate the parameters of the cascades γ-decay to a precision achieved in the experiment. For example, it overestimates level density at $E_{ex} \sim 0.5B_n$ by the order of magnitude. At the same time, the estimated (Fig. 5) sums of radiative strength functions of $E1$ and $M1$ transitions also differ from the predictions of the sufficiently simple models [17-19], which are usually used for calculation of such parameters as, for example, the total radiative width.

4 Analysis

4.1 Total intensities of two-step cascades at different excitation energies

From the coincidences stored in the experiment, it is very simple to construct an intensity distribution of the two-step cascades which includes both primary and secondary transitions. Quanta ordering for the majority of the intense cascades whose parameters are given in Tables 1 and 2 was determined the [11] under obvious condition that the primary transitions in different cascades proceeding via the same intermediate level have the same energy in different spectra; secondary transitions of these cascades have different energies. As follows from Table 3, the main part of the intensity corresponding to the excitation of levels below $\sim$ 3.5 MeV was established in the experiment. Subtracting this part of the intensity from the experimental distributions, we get the intensity of the cascades which excit higher-lying levels. Thus, as was first suggested in [6], one can

determine the dependence of cascade intensities on the energy of their intermediate levels for practically the total excitation interval $E_{ex} \simeq B_n$.

Such a dependence for ^{168}Er, obtained after summation of the cascade intensities over all final levels and in energy intervals $\Delta E = 0.5$ MeV, is shown in Fig. 3. Experimental data (histograms) are compared with two variants of the calculations. The shape of the dependence of level density on nuclear excitation energy in the first variant was determined within model [14] and in the second variant, within model [22]. Both variants used conventional models [17-19] to describe the radiative widths. As can be seen from this figure, the calculation based on the Fermi-gas level density model [14] (curve 1) cannot correctly predict the intensity of cascades at sufficiently high excitations of ^{168}Er. This situation is typical for any deformed nucleus from the region of the 4s-resonance of the neutron strength function. A possible explanation of this effect directly follows from an analysis of notions of a nucleus in framework of which the models [14] and [22] were developed. Model [22] sufficiently realistic accounts for co-existence and interaction of vibrational and quasiparticle excitations above the 4 MeV excitation energy of the nucleus under study. However, at the lower excitation energy adiabatic approach (basis of model [22]), probably, does not correspond to reality. Results of the analysis [23] testify to possible dominant influence of vibrational-type components of wave functions of the states of even-even deformed nuclei at $E_{ex} \leq B_n$.

4.2 Factors determining level density at low excitations

Figure 4 shows the number of cascade intermediate levels in the 100 keV energy interval as a function of the excitation energy. Experimental data (points) are compared with the predictions of the conventional back-shifted Fermi-gas model [14] and model [22]. As can be seen from this figure, the modern notions of a nucleus [22] reproduce experimental data only above 4 MeV. Probable level density below 4 MeV is not reproduced within any existing model. A possible explanation of this situation can be obtained from an analysis of spacings between the intermediate levels (or their multiplets) of the most intense cascades. The algorithm of this analysis is described in [23] and some its results concerning ^{168}Er are given below.

Figure 6 demonstrates the absolute intensity of all two-step cascades placed in the decay scheme smoothed by the Gaussian function with the parameter $\sigma = 25$ keV (see Tables 1 and 2). These are shown separately for cascades terminating at the levels of the γ-band and the band of the ground state. As seen from the figure, the spacings between the most intense peaks in this distributions are almost equal. These peaks can be placed in practically equidistant "bands", the search for which was performed by means of the autocorrelation function

$$A(T) = \sum_E F(E) \times F(E+T) \times F(E+2T). \qquad (3)$$

The values of the autocorrelation function versus the equidistant period T are shown in Fig. 7. It follows from this figure that, indeed, one or more groups consisting of at least 3 intermediate levels (or their close doublets) for the strongest cascades terminating at levels of the γ-band appear in ^{168}Er. These groups are marked in Fig. 6. It should be noted that the problem considered here cannot have unique solution, even in principle [24], if only

the ensemble of cascades following thermal neutron capture in a single nucleus is involved in the analysis. An unambiguous proof for the presence of the observed regularity can be obtained only after studying the two-step cascades in a number of resonances of the ^{167}Er target-nucleus.

Nevertheless, using the data on the equidistant periods [23] for nuclei studied by us earlier, one can choose the value $T = 740$ keV as the most probable equidistant period for ^{168}Er. The dependence of the probable equidistant periods on the number N_b of the boson pairs in the unfilled nuclear shells for the group of N-even nuclei in which two-step cascades were studied is shown in Fig. 8.

5 Conclusions

The analysis of the experimental data on the two-step cascades proceeding between the compound state and a group of low-lying levels of ^{168}Er shows that the γ-decay process of this nucleus reveals the same main peculiarities as those observed earlier for the deformed nuclei. These results support previous assumptions about the factors affecting the γ-decay:

(a) the sharp change in nuclear properties at the excitation energy of 3-4 MeV;

(b) the possible dominance of vibrational-type excitations below this energy, which results in a strengthening of the widths of the cascade transitions to the low-lying levels of the nucleus under study. The greatest strengthening can be related to the practically harmonic nuclear vibrations having a phonon energy of 700-750 keV, as well as a considerable decrease in the number of excited states in the energy interval from 2 to 4 MeV.

Acknowledgments

Authors thanks are due to Ms. Ann Schaeffer for her help in preparation of the English version of this paper.

This work was supported by RFBR Grant No. 95-02-03848.

Table 1.

A list of absolute intensities (per 10^4 decays), $i_{\gamma\gamma}$, of measured two-step cascades and energies, E_2 of their secondary transitions for ^{168}Er. i_1 and i_2 are relative intensities of primary and secondary cascade transitions according to [1,2], respectively. E_i is the energy of intermediate level with $J^\pi K$. J_f is the spin of the final state of cascade transitions.

E_i,keV	$J^\pi K$	J_f	E_1, keV	E_2, keV	$i_{\gamma\gamma}$	i_1	i_2	$i_{\gamma\gamma}/i_1$, %	$i_{\gamma\gamma}/i_2$, %
821.17	2^+2	2	6950.2	741.36	2.8(5)	4.4	491	64(15)	0.6(2)
895.79	3^+2	2	6875.3	815.99	2.5(4)	1.2	3000	200(40)	0.08(2)
994.75	4^+2	4	6776.6	730.66	1.8(4)	1.6	831	112(30)	0.22(5)
1117.57	5^+2	4	6663.5	853.47	1.3(4)	1.0	518	130(40)	0.25(9)
1193.03	5^-4	4	6578.4	928.94	1.8(5)	22	110	8(3)	1.6(5)
1276.27	2^+0	2	6495.1	1196.51	1.9(5)	7.6	52	25(8)	3.7(10)
		4		1012.19	2.9(5)		99	38(7)	2.9(5)
1403.74	2^-1	2	6367.42	1323.91	10.5(11)	14.6	124	72(8)	8.5(8)
		2γ		582.57	2.1(8)		37	14(8)	5.7(24)
1411.10	4^+0	2	6360.4	1331.32	-	18.4	112	-	-
		4		1147.00	-		74	-	-
		3γ		862.36	2.7(8)	-	72	15(6)	3.8(11)
1431.47	3^-1	2	6339.9	1351.54	2.4(6)	3.8	133	63(16)	1.7(5)
		4		1167.40	1.3(6)		130	34(17)	1.0(5)
1493.14	2^+0	4	6278.2	1229.08	1.3(6)	0.7	41	180(90)	3.2(15)
1541.56	3^-3	4	6229.7	1277.45	< 4.2	40	16	-	< 30
		2γ		720.39	6.5(11)		110	> 16	6(1)
		3γ		645.78	< 4.6		35	-	< 0.13
		4γ		546.80	< 3.3		23	-	< 0.14
1541.71	4^-1	4	6229.7	1277.59	< 4.2	40	141	-	< 0.03
		3γ		645.94	< 4.6		24	-	< 0.2
		4γ		546.96	< 3.3		40	-	< 0.1
1569.45	2^-2	2γ	6202.1	748.28	4.7(14)	10.4	86	45(14)	0.054(20)
		3γ		673.67	4.0(13)		38	38(13)	0.10(3)
1574.12	5^-1	4	6197.42	1310.03	8.6(9)	13.8	123	62(7)	0.070(7)
		6		1025.38	5.8(11)		70	42(4)	0.083(16)
1615.34	4^-3	3γ	6155.8	719.55	-	21.6	78	-	-
1633.46	3^-2	2γ	6137.8	812.29	< 23	38.8	69	< 60	< 0.3
		3γ		737.69	< 31	-	82	< 80	< 37
		4γ		638.71	9(2)	-	55	< 80	0.16(4)
1656.27	4^+0	2	D: 6116.9+	1576.58	1.0(4)	6.4	< 6	16(7)	> 0.17
		4	6113.5	1392.21	1.5(5)		98	23(6)	0.015(5)
1719.18	4^-2	3γ	6151.96	823.39	< 40	30.2	85	< 130	< 0.9
		4γ		724.43	< 10		33	< 30	< 0.3

Table 1 (continue)

E_i,keV	$J^\pi K$	J_f	E_1, keV	E_2, keV	$i_{\gamma\gamma}$	i_1	i_2	$i_{\gamma\gamma}/i_1$, %	$i_{\gamma\gamma}/i_2$, %
1736.68	4^+3	4γ	6034.7	741	5.1(16)	5.8	< 491	88(28)	> 1
1828.06	3^-3	3γ	5943.3	932.27	8.4(20)	13.5	51	62(13)	16(4)
		4γ		833.29	4(1)		32	30(8)	13(4)
1892.94	4^-3	4^-	5878.34	798.89	50(3)	54	160	93(6)	31(2)
1905.09	4^-4	4^-	5866.4	811.04	< 30	10.9	115	< 300	< 30
1913.90	3^-0	2	5857.6	1834.05	< 8.6	19.8	40	< 43	< 43
		4		1649.77	6.9(19)		50	35(10)	14(5)
1915.50	3^+2	2	5857.6	1835.68	< 8.6	19.8	58	< 43	< 15
		2γ		1094.4	1.7(6)		12	8.5(30)	14(5)
		4γ		920.78	4.6(9)		14	23(5)	33(7)
1930.39	2^+2	2	5841.2	1850.46	1.4(5)	1.2	22	116(50)	6(2)
1972.93	2^-1	2	5799.2	1892.73	1.5(5)	2.6	30	58(20)	5(2)
1994.82	3^+2	2	5777.6	1914.97	3.1(6)	23	40	13(3)	8(2)
		4		1730.89	2.2(7)		18	10(3)	12(4)
2022.33	3^-3	2	5748.8	1942.69	8.4(9)	11.1	64	76(8)	13(2)
		4		1758.47	2.0(7)		18	18(7)	7(2)
		4^-		928.29	5.0(2)		110	45(2)	5(2)
2031.09	4^+0	4	5740.3	1766.99	1.3(5)	2.2	42	59(23)	3(1)
2059.98	4^-4	4^-	5711.4	965.94	7.4(18)	10.5	65	70(20)	11(2)
2088.42	4^-3	4	5682.0	1825	1.8(9)	7.6	-	24(12)	-
		4γ		1093.67	1.8(9)		5	24(12)	36(20)
2097.57	4^-1	4	5673.7	1833.43	6.2(12)	25.2	38	25(5)	16(3)
		3γ		1201.76	8.5(17)		26	34(7)	33(7)
2129.24	5^-0	4	5642.0	1865.10	9.7(11)	13.5	40	72(8)	24(3)
		6		1580.72	7.4(14)		38	55(11)	19(4)
2148.37	5^-4	4	5623.1	1883.47	2.2(7)	11.5	7	19(7)	31(10)
2188.38	4^+	6	5585.7	1639.73	5.1(13)	5.2	7	100(20)	73(19)
2200.42	5^-3	4	5571.0	1936.4	2.0(7)	14.1	< 30	14(5)	> 66
		6		1651.5	4.3(11)		< 7	30(8)	> 61
2238.18	4^+4	4^-	5533.2	1144.11	4.5(18)	5.3	59	85(4)	8(3)
2262.70	3^-3	2γ	5508.6	1441.41	1.5(7)	9.3	19	16(8)	8(4)
		3γ		1366.91	3.9(13)		23	42(15)	17(6)
2267.62	5^+	4^-	5503.6	1173.56	8.4(23)	8.9	47	94(26)	18(5)
2302.68	3^-	2	5468.8	1481.71	2.2(7)	10.4	10	21(8)	22(8)
		4γ		1309	3.3(10)		< 123	32(11)	> 27
2311.07	4^+	4	5460.2	2047.03	4.7(10)	5.8	47	81(19)	10(2)

Table 1 (continue)

E_i,keV	$J^\pi K$	J_f	E_1, keV	E_2, keV	$i_{\gamma\gamma}$	i_1	i_2	$i_{\gamma\gamma}/i_1$, %	$i_{\gamma\gamma}/i_2$, %
2336.26	4^+	3γ	5434.3	1440.41	< 4.1	15.3	10	< 27	< 40
		4γ		1341.58	3.8(9)		11	25(7)	35(6)
2337.13	3^-	2	5434.3	2256.7	1.2(5)	15.3	17	8(3)	7(3)
		2γ		1515.98	3.0(8)		< 20	20(6)	> 15
		3γ		1441.42	< 4.1		< 15	< 27	-
2365.17	5^-5	4^-	5405.9	1271.13	14(3)	12.0	29	117(30)	48(10)
2392.63	4^-2	4γ	5378.7	1398.05	5.2(13)	11.7	12	44(12)	43(12)
		4^-		1298.40	< 10		7.2	< 85	< 140
2393.63	2^+	2	5378.7	2314.49	1.3(6)	11.7	14	11(6)	9(5)
2398.55	(5)	6	5373.2	1850	7.1(24)	12.7	< 22	56(20)	> 32
		4^-		1302	< 10		-	< 80	-
2402.38	4^-	3γ	5369.2	1506.49	15(3)	20	18	75(25)	83(20)
		4γ		1407.67	5.8(11)		7	29(5)	83(17)
		4^-		1308	7.2(20)		< 120	36(10)	> 6
2411.64	4^-	2	5359.7	2147.34	1.1(5)	48	< 7.2	23(11)	> 15
		3γ		1515.98	23(8)		51	48(16)	45(17)
		4γ		1417.05	4.3(11)		5 from 15	9(3)	~ 86
		4^-		1317.56	< 19		5	< 40	< 38
2423.24	4	4	5348.1	2159.15	7.1(10)	6.7	35	106(15)	20(3)
2437.13		4	5336.7	2137.04	2.0(7)	1.6	-	125(40)	-
2451.18		4^-	5320.5	1358	4.6(20)	5.4	< 10	85(40)	> 46
2477.13	5^-	6	5295.8	1928.21	12(2)	42	16	29(5)	75(20)
2478.09	3^-	2	5292.6	2398.25	1.5(5)	42	< 18	4(2)	> 8
		4		2214.47	8.9(12)		13	21(4)	68(10)
		2γ		1656.84	5.4(9)		< 8	13(3)	> 68
		3γ		1582.96	9.4(19)		9	22(5)	100(20)
		4γ		1484.46	10.2(15)		17	24(4)	60(10)
2494.02	(3^-)	2	5277.4	2414.33	3.1(7)	11.6	8	27(7)	39(10)
		4		2229.27	2.5(8)	-	5	22(8)	50(17)
		2γ		1672.84	5.0(8)		19	43(8)	26(4)
2513.70	(5^-)	4γ	5258.6	1518.95	2.2(8)	12.7	9	17(7)	24(9)
2528.69	$(3-5)^-$	4γ	5242.5	1534.05	6.5(11)	13.2	21	49(8)	31(6)
2551.5		4γ	5218.7	1556.84	4.4(18)	6.9	27	64(30)	16(7)
2559.6	(5^-)	4γ	5212.5	1563.85	4.6(17)	19.3	15	24(8)	31(12)
2571.3		3γ	5200.0	1675.49	3.9(14)	9.7	20	40(15)	20(7)
		4γ		1576.58	4.0(14)		< 6	41(15)	> 67
2601.5		2	5169.9	2522	12(2)	36	-	33(6)	-
		4		2337.1	13(2)		16	36(6)	81(12)
		6		2052	3.6(12)		-	10(3)	-

Table 1 (continue)

E_i,keV	$J^\pi K$	J_f	E_1, keV	E_2, keV	$i_{\gamma\gamma}$	i_1	i_2	$i_{\gamma\gamma}/i_1$, %	$i_{\gamma\gamma}/i_2$, %
2629.5		4	5141.8	2365.30	1.8(7)	5.8	13	31(12)	14(5)
2656.7	(3^-)	2γ	5114.6	1835.68	8.2(10)	14.5	< 58	57(7)	> 14
		3γ		1762.19	9.6(22)	-	< 13	66(15)	> 74
2659.8	(3^-)	2	5111.5	2580	4.8(8)	19.1	-	25(4)	-
		4		2395	2.1(8)		-	11(4)	-
		3γ		1765.02	6.1(15)		10	32(8)	61(15)
		4γ		1665.74	5.4(11)		8	28(6)	68(14)
2673.6		4	5097.7	2410	3.8(9)	5.4	< 14	70(17)	> 27
2683.5		4	5087.6	2420	4.5(8)	4.8	< 16	94(17)	> 28
2700.5		4	5070.8	2436.49	6.3(10)	15.9	15	40(6)	42(7)
2733.4	$(3,4^-)$	4	5038.2	2469	4.7(18)	24	-	20(8)	-
		3γ		1837	8.4(19)		-	35(8)	-
2739.1	$(3,4^-)$	4	5032.2	2475	1.9(6)	12	15	16(5)	13(4)
2746.5		2γ	5024.8	1925	2.0(6)	2.6	< 20	77(23)	> 10
2769.58		4^-	5001.6	1675.49	7.2(20)	12.5	20	58(16)	36(10)
2777.5	(5^-)	6	4993.8	2229.27	4.1(14)	6.0	5	68(23)	82(28)
2786.9	$(3,4^-)$	4	4984.5	2524.0	7.5(12)	14.7	< 28	51(8)	> 27
		3γ		1890.9	7.5(13)		4	51(9)	187(33)
2790.8		4	4980.5	2524	7.5(13)	4.2	8	178(31)	94(16)
2810.9		4	4960.4	2547	3.1(8)	3.3	-	94(24)	-
2819.7		4	4951.7	2556	4.0(10)	2.2	-	181(45)	-
2849.8		2	4921.6	2770	2.5(10)	46	-	5.4(21)	-
		4		2586	5.3(10)		-	11(2)	-
		6		2300.63	26(3)		34	57(7)	76(9)
		2γ		2029	3.3(8)		< 7	7(2)	> 47
		3γ		1954	5.5(18)		< 6	12(4)	> 92
		4γ		1855.6	4.8(12)		3	10(3)	160(40)
		4^-		1756	8(2)		< 10	17(4)	> 80
2875.2	4^-	4	4896.4	2611	3.8(10)	12.7	-	30(8)	-
		4γ		1880.47	3		3	-	-
2890.2		6	4881.1	2341.89	5.0(15)	4.4	12	114(34)	42(13)
2895.4		2	4875.9	2815	2.8(9)	3.9	-	72(23)	72(23)
		4		2631	2.8(9)		-	72(23)	-
2920.0		4	4851.4	2656	3.6(10)	5.0	-	22(20)	-
2933.2	(3^-)	2	4838.1	2853	2.7(12)	8.6	-	31(14)	-
		4		2669	5.0(10)		-	58(12)	-
		4γ		1938.69	4.5(14)	-	10	52(16)	45(14)
		4^-		1839	13.0(25)		< 20	151(29)	> 26

Table 1 (continue)

E_i,keV	$J^\pi K$	J_f	E_1, keV	E_2, keV	$i_{\gamma\gamma}$	i_1	i_2	$i_{\gamma\gamma}/i_1$, %	$i_{\gamma\gamma}/i_2$, %
2950.0		2	4820.7	2820	3.2(12)	4.2	-	76(28)	-
		4		2686	4.1(10)		-	-	-
2969.6	(5^-)	6	4801.7	2420	2.9(13)	20.4	< 16	14(7)	> 8
2972.6		2	4798.8	2893	2.8(10)	2.9	-	97(30)	-
2979.3		2γ	4792.1	2158	2.9(10)	3.9	< 10	74(25)	> 30
2991.3	(3^-)	2	4780.0	2911	3.2(10)	10	-	32(10)	-
2998.2		4	4773.2	2734	3.2(10)	7	-	46(16)	-
3011.8		2	4759.5	2932	5.0(12)	10.5	-	48(11)	-
		4		2747	6.9(12)		-	-	-
		6		2462	8.6(17)		-	-	-
		2γ		2189	2.4(10)		< 5	-	> 48
3026.0	(5^-)	6	4745.4	2472.2	14.9(21)	18	15	83(12)	100(20)
3030.5		4	4740.9	2769	3.8(9)	5.4	-	70(17)	-
3033.8		2γ	4737.6	2212.7	3.3(11)	2.6	8	127(42)	41(14)
3042.1		4^-	4729.2	1948.72	2.8(11)	3.6	4	78(30)	70(28)
3049.6		2	4721.7	2970	3.4(12)	6.8	-	50(18)	-
		2γ		2229.27	2.7(10)		5	37(15)	54(20)
3068.8		6	4702.5	2520	6.1(16)	5.4	-	113(30)	-
3082.8		2	4688.5	3003	3.2(12)	10.2	-	31(12)	-
		4		2819	4.3(15)		-	42(15)	-
		6		2533	2.6(15)		-	25(15)	-
3099.42	(3^-)	2γ	4671.4	2277.97	-	13.5	6	-	-
		3γ		2203.65	-		19	-	-
		4γ		2104.67	5.3(13)		8	39(10)	66(16)
3111.25	(3^-)	2	4660.0	3031	3.3(9)	13.5	-	24(7)	-
		2γ		2290	4.2(11)		< 5	31(8)	> 84
		3γ		2214.47	8(3)		< 13	59(22)	> 61
		4γ		2116.48	4.1(14)		9	30(10)	45(16)
3118.2		4	4653.2	2860	7(3)	16.9	-	43(18)	-
3124.0		6	4674.4	2575	13(8)	12.4	-	105(65)	-
		2γ		2303.22	6.5(13)		12	52(10)	54(11)
3127.9	(5^-)	4	4643.4	2864	11(3)	23.8	-	46(13)	-
		6		2579	6.7(8)		-	28(4)	-
3142.7	(3^-)	2	4628.7	3063	2.0(9)	14.6	-	14(6)	-
		4		2879	3.7(14)		-	25(10)	-

"<" denotes intensities of transitions and cascades in the case of unresolved doublet (for the cascade — at presence of unresolved doublet of primary transitions or due to the possible registration of its primary and secondary quanta); the intensity of unresolved primary transition is given for revealed doublets of close levels.

Table 2.

Absolute intensities (per 10^4 decays of the ^{168}Er compound nucleus) of the two-step cascades. E_1 is the energy of the primary cascade transition exciting intermediate level at the energy E_i. J_f is the spin of the final state of cascade.

E_1, keV	E_i, keV	J_f	$i_{\gamma\gamma}$	E_1, keV	E_i, keV	J_f	$i_{\gamma\gamma}$
5958.8	1812.2	2γ, 3γ, 4γ	22(3)	4263.6	3507.4	2	3(1)
5694.7	2076.3	4^-	10(2)	4257.5	3513.5	6	8(2)
5552.8	2218.2	3γ	5.7(17)	4250.3	3520.7	2	2.4(8)
5055.3	2715.7	2, 4	5.6(12)	4211.4	3559.6	6	5(2)
4619.5	3151.5	2γ	3.4(1)	4200.5	3570.5	6, 2γ,3γ	15.(3)
4613.1	3157.9	2	2.6(8)	4183.4	3587.6	4γ	3.7(14)
4573.4	3197.6	2	4.3(9)	4164.6	3606.4	2	1.7(8)
4566.2	3204.8	4	6.1(14)	4153.6	3617.4	2, 2γ, 4γ	9(2)
4548.2	3222.8	4, 6, 2γ	14(3)	4128.3	3642.7	2γ	3(1)
4533.4	3237.6	4	4.1(14)	4110.5	3660.5	2γ	4(1)
4486.3	3284.7	2, 4, 6	14(3)	4091.3	3679.7	2γ, 4γ	8(2)
4444.1	3326.9	2	3.2(8)	4068.9	3702.1	2	1.7(8)
4436.4	3334.6	6, 3γ	12(3)	4056.2	3714.8	3γ	7(2)
4423.7	3347.3	4γ	5.0(15)	4032.4	3738.6	2γ, 4^-	11(3)
4394.8	3376.2	2, 6, 2γ	12(2)	4016.0	3755.0	3γ	9(2)
4376.9	3394.1	4^-	7(2)	4009.8	3761.2	2γ	4(1)
4372.1	3398.9	2	3.0(8)	3989.7	3781.3	4, 6, 4γ	16(3)
4355.9	3415.1	2	3.3(8)	3972.0	3799.0	6	4.3(18)
4339.4	3431.6	2, 6	7(2)	3954.4	3816.6	2γ	3.6(14)
4295.7	3475.3	2	3.6(8)	3936.2	3834.8	4	3(1)
4284.1	3486.9	3γ	6(2)	3883.0	3888.0	3γ	7(2)
4275.0	3496.0	2, 6	10(2)	3876.2	3894.8	4	5(1)
4272.1	3498.9	4^-	9(3)	3863.1	3907.9	4	4(1)

Table 3.

The summed experimental, $\sum i^{exp}$, and modelled, $\sum i^{mod}$, intensities (in % per decay) for two-step cascades or primary transitions. L_c is the detection threshold for the cascade, i_{max} is maximum value of the intensity which limits the interval of comparison, N_i^{mod} is the number of intermediate levels excited by dipole primary transitions (under the assumption of an equality of level densities for both parities), Δ is the ratio of $E1$ and $M1$ transitions which provides the best correspondence between experimental and calculated distributions. Here, δi and δN are the mathematical expectations of unobserved intensities and the number of levels corresponding to the sum of low-intensity ($i < L_c$) parts of two Porter-Thomas distributions with $\nu = N_i^{mod}$ for each, $< \rho \times \Delta E >$ is the number of levels, predicted according to [13], excited by primary $E1$ transitions after decay of the ^{168}Er compound state with $J^\pi = 4^+$ in the excitation energy interval considered here.

Interval	1.5-2.0 MeV		2.0-2.5 MeV		2.5-3.0 MeV		3.0-3.5 MeV	3.5-4.0 MeV
for:	$(n,2\gamma)$	(n,γ)	$(n,2\gamma)$	(n,γ)	$(n,2\gamma)$	(n,γ)	$(n,2\gamma)$	$(n,2\gamma)$
$\sum i^{exp}$, %	3.5	3.3	3.53	3.79	3.11	4.5	2.94	1.39
$\sum i^{mod}$, %	3.65	3.5	4.0	5.0	3.3	5.2	3.3	1.8
L_c, %	0.015	0.012	0.015	0.016	0.02	0.017	0.02	0.024
i_{max}, %	0.3	0.3	0.3	0.3	0.3	0.3	0.3	0.3
N_i^{mod}	12	17	23	42	47	63	38	40
Δ	0.18	0.25	0.4	0.2	0.35	0.21	0.37	0.36
δi, %	0.04	0.04	0.1	0.2	0.3	0.4	0.3	0.4
δN,	7	7	14	36	51	64	39	53
$< \rho \times \Delta E >$	8	8	26	26	76	76	203	159

The Δ value obtained for the $(n,2\gamma)$ reaction should be with a higher probability related to the ratio of the intensities of cascades with primary $E1$ transitions to those with primary $M1$ transitions.

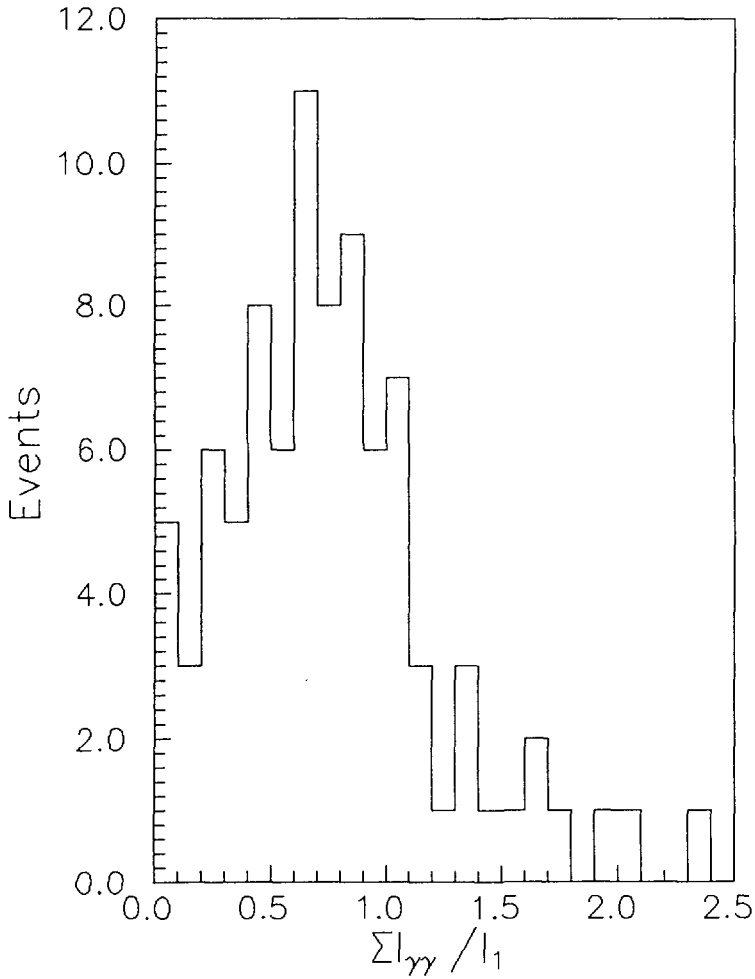

Fig. 1. Frequency distribution of the ratios, $r = \sum i_{\gamma\gamma}/i_1$, of the sum cascade intensities to the intensities of their joint primary transitions.

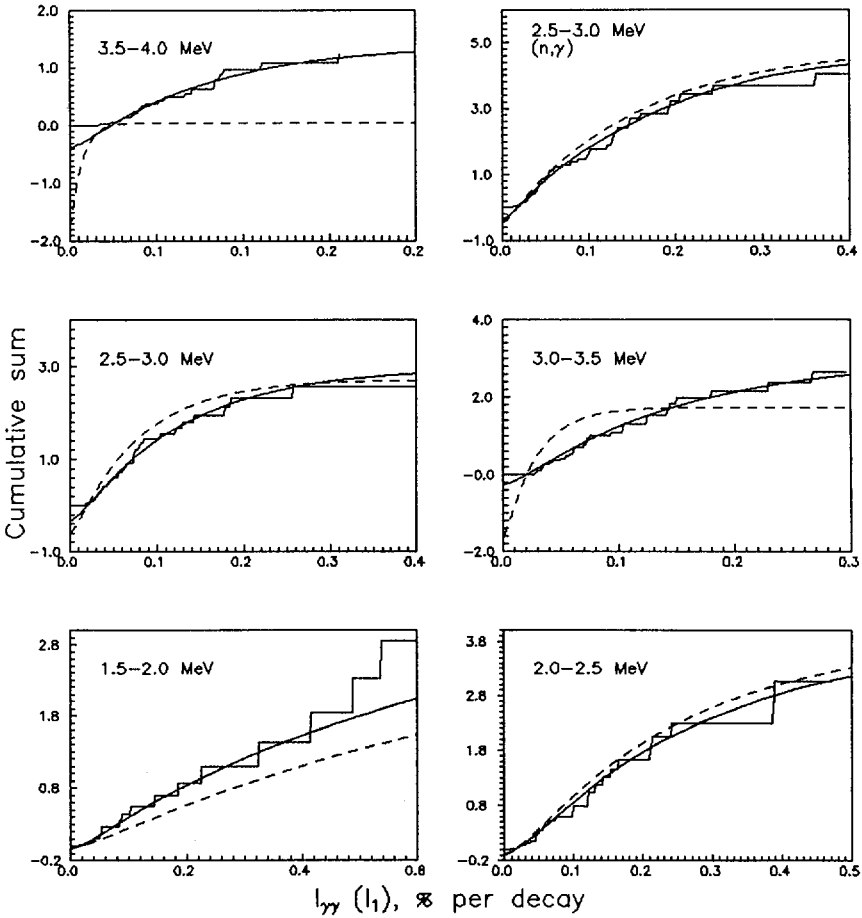

Fig. 2. Cumulative sums of the cascade intensities (primary transitions) for excitation energy intervals of 0.5 MeV in the diapason from 1.5 to 4.0 MeV versus the running value of the intensity. The histograms represent the experimental data and curves visualize simulations within the Porter-Thomas distributions: solid curve corresponds to a distribution with the parameters providing the best description of the experiment, dashed curve represents the distribution for the same total cascade intensity, but for the level density predicted by the BSFG model [14].

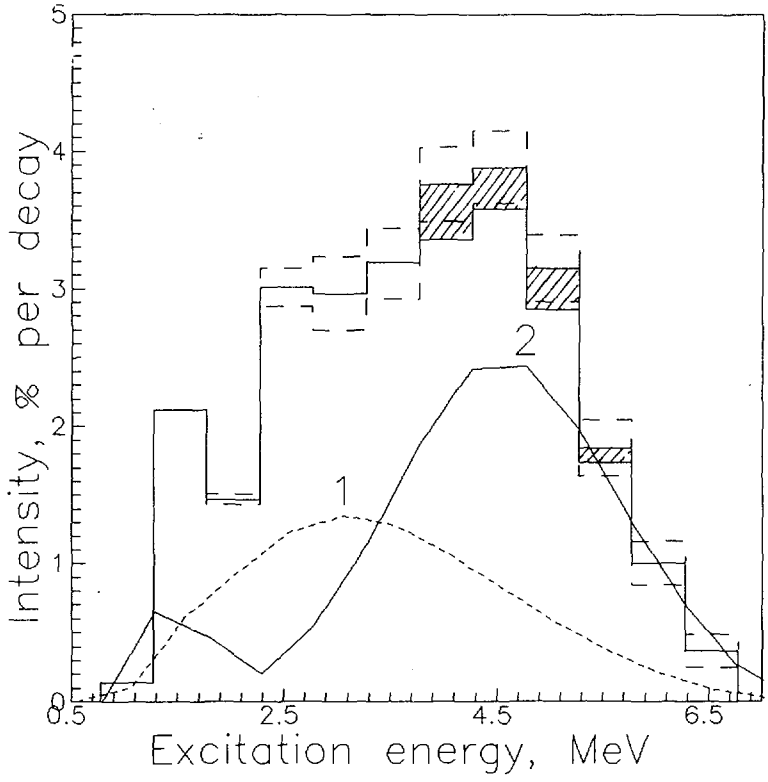

Fig. 3. Total two-step cascade intensities (in % per decay) as a function of excitation energy. The histograms represent the experimental intensities (summed in energy bins of 500 keV) with ordinary statistical errors; the maximum possible estimates of probable systematic errors (the δi values from Table 3) are shown by black rectangles. Curves 1 and 2 correspond to predictions according to models [14] and [22], respectively.

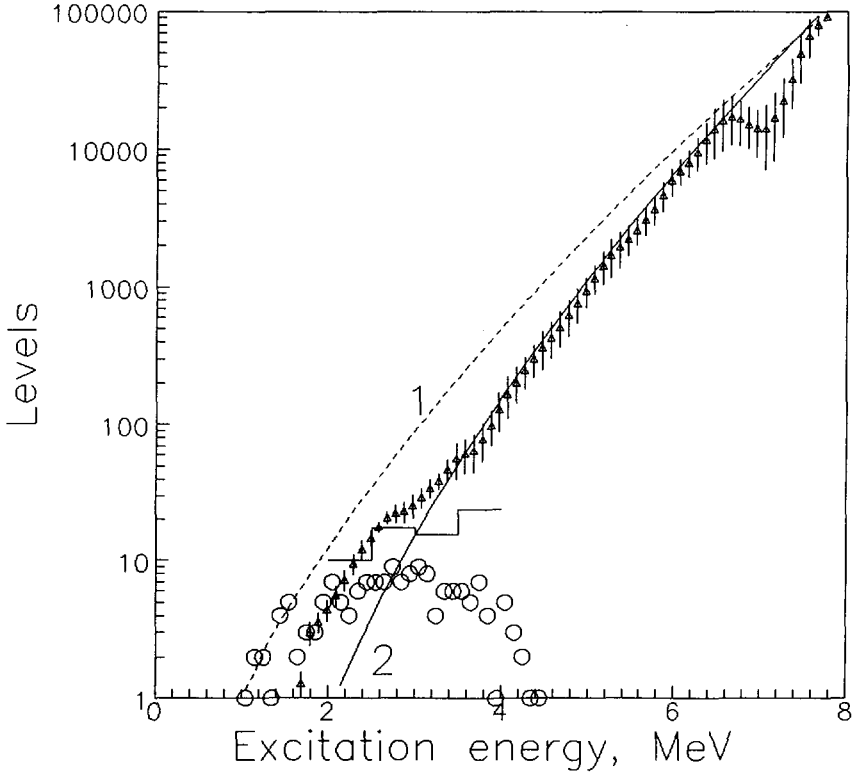

Fig. 4. Number of observed levels of the most intense cascades in ^{168}Er (Tables 1 and 2) for an excitation energy interval of 100 keV (points). Curves 1 and 2 represent the predictions of models [14] and [22], respectively. Histogram is the estimation [13] of level density from the shape of distribution of the cumulative sums of cascade intensities. Triangles with bars represent level density providing simultaneous reproduction in the calculations of both Γ_λ and $I_{\gamma\gamma}$.

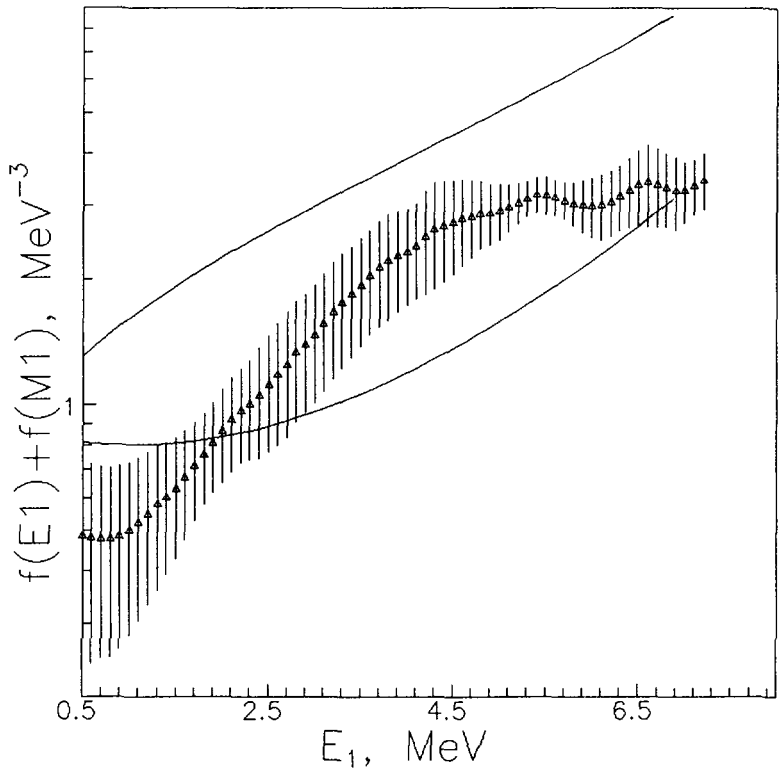

Fig. 5. The interval of probable values of the sum strength functions for $E1$ and $M1$ transitions (multiplied by 10^9) providing correspondence between the experimental and calculated values of Γ_λ and $I_{\gamma\gamma}$. The upper curve represents calculations according model [18] and under assumption $f(M1) = const$, the lower curve is the same for model [17].

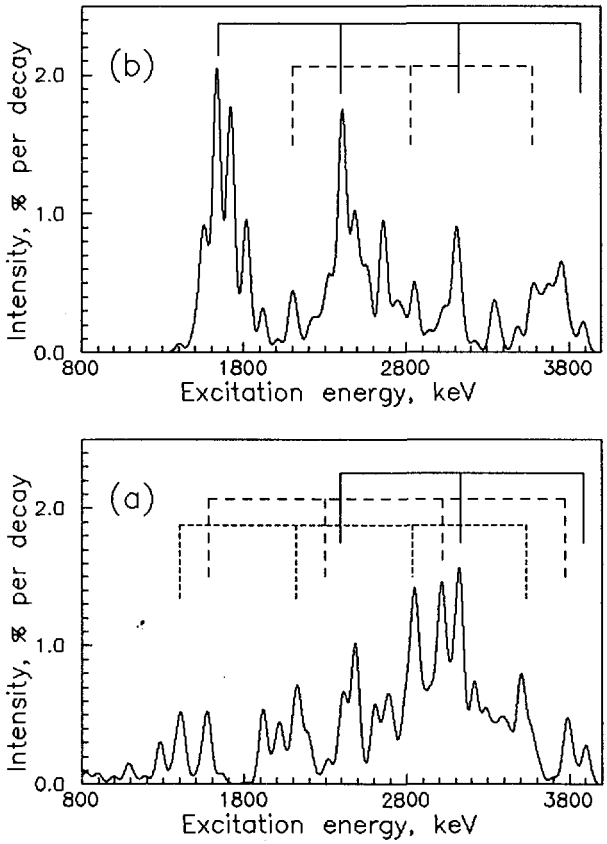

Fig. 6. The dependence of the intensities (% per decay) of the resolved cascades listed in Tables 1 and 2 on the excitation energy. Possible "bands" of practically harmonic excitations of the nucleus are marked. The "smoothing" parameter $\sigma = 25$ keV was used. (a) — for cascades to levels of the band of the ground state, (b) — to levels of the γ-band.

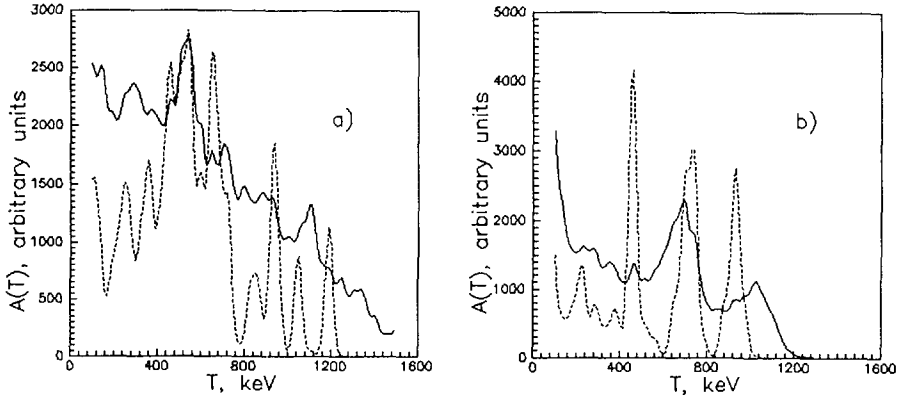

Fig. 7. The values of the functional $A(T)$ for the two registration thresholds of the most intense cascades: the solid curve corresponds to all resolved cascades listed in the tables; the dashed curve corresponds to cascades with intensities higher than 0.1% per decay. Notations are the same as in Fig. 6.

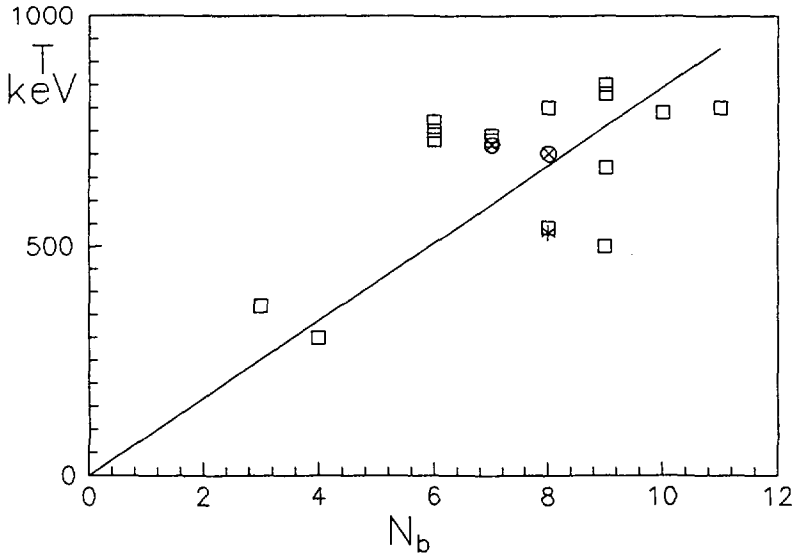

Fig. 8. The values of the equidistant period, T, for ^{177}Lu (asterisk) and even-even nuclei studied earlier (rectangles) as a function of the number of boson pairs, N_b, in the unfilled shells. The $\otimes$ show the ϵ_d values for the $^{110,112}Cd$ nuclei. Line extrapolates the possible dependence.

References

[1] W. F. Davidson et al., J. Phys. G., Nucl. Phys. **17** (1991) 1683;
[2] V. S. Shirley, Nuclear Data Sheets **71** (1994) 455;
[3] V. G. Soloviev et al., J. Phys. G., Nucl. Phys. **20** (1994) 113;
[4] A. Jungclaus, Phys. Rev. C. **49** (1994) 88;
[5] R. L. Gill et al., Phys. Rev. C **54** (1996) 2276;
[6] S. A. Berendakov at al., Yad. Phys. **V.61(3)** (1998) 232;
[7] S. T. Boneva et al., Izv. AN SSSR, Ser. Fiz. **55(5)** (1991) 841;
[8] S. T. Boneva, E. V. Vasilieva, Yu. P. Popov, A. M. Sukhovoj and V. A. Khitrov, Sov. J. Part. Nucl. **22(2)** (1991) 232;
[9] S. T. Boneva et al., Sov. J. Part. Nucl. **22(6)** (1991) 698;
[10] A. M. Sukhovoj and V. A. Khitrov, Sov. J.: Prib. Tekhn. Eksp. **5** (1984) 27;
[11] Yu. P. Popov, A. M. Sukhovoj, V. A. Khitrov and Yu. S. Yazvitsky, Izv. AN SSSR, Ser. Fiz. **48** (1984) 1830;
[12] C. F. Porter and R. G. Thomas, Phys. Rev. 104(2) (1956) 483;
[13] A. M. Sukhovoj and V. A. Khitrov, Sov. J. Yad. Fiz., 1997;
[14] W. Dilg, W. Schantl, H. Vonach and M. Uhl, Nucl. Phys. **A217** (1973) 269;
[15] V. A. Khitrov, A. M. Sukhovoj, Proc. of VI International Seminar on Interactions of Neutrons with Nuclei (Dubna, 1998) E2-98-202, Dubna (1998) 172;
[16] S.F.Mughabghab, Neutron Cross Sections. V. 1. Part B. N.Y. Academic Press, (1984);
[17] S. G. Kadmenskij, V. P. Markushev and W. I. Furman, Sov. J. Nucl Phys. **37** (1983) 165;
[18] P. Axel, Phys. Rev. **126(2)** (1962) p.671;
[19] J. M. Blatt and V. F. Weisskopf, Theoretical Nuclear Physics, New York (1952);
[20] S. T. Boneva, V. A. Khitrov, A. M. Sukhovoj and A. V. Vojnov, Z. Phys.- A **338** (1991) 319;
[21] S. T. Boneva, V. A. Khitrov, A. M. Sukhovoj and A. V. Vojnov, Nucl. Phys. **A589** (1995) 293;
[22] A. V. Ignatyuk, Proc. IAEA Consultants meeting on the use of Nuclear Theary in Beutron Nuclear Data Evaluation (Trieste, Italy, 1976, IAEA-190, Vol. 1) p.211;
[23] V. A. Khitrov and A. M. Sukhovoj, Izv. RAN., ser. fiz., **61(11)** (1997) 2068;
[24] E. V. Vasilieva et al., Bulletin of the Russian Academy of Science, Physics **57** (1993) 1582;

Received by Publishing Department
on May 12, 1999.